

UC San Diego

UC San Diego Previously Published Works

Title

Synthesis and Performance of L-Tryptophanamide and (S)-1-(Naphthalen-2-yl)ethanamine-Based Marfey-Type Derivatives for Amino Acid Configurational Analysis: Diastereomeric Resolutions Directed by π -Cation Bonding.

Permalink

<https://escholarship.org/uc/item/32x6223r>

Journal

Journal of Organic Chemistry, 90(9)

Authors

Salib, Mariam

Molinski, Tadeusz

Publication Date

2025-03-07

DOI

10.1021/acs.joc.4c02882

Peer reviewed

Synthesis and Performance of L-Tryptophanamide and (S)-1-(Naphthalen-2'-yl)ethanamine-Based Marfey-Type Derivatives for Amino Acid Configurational Analysis: Diastereomeric Resolutions Directed by π -Cation Bonding

Mariam N. Salib and Tadeusz F. Molinski*



Cite This: *J. Org. Chem.* 2025, 90, 3269–3278



Read Online

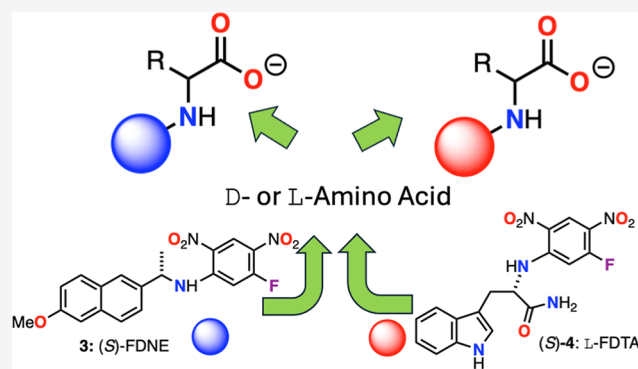
ACCESS |

Metrics & More

Article Recommendations

Supporting Information

ABSTRACT: The configurational analysis of amino acids (AAs) in natural product peptides, often containing nonproteinogenic AAs, is mostly carried out by the venerable Marfey's method using a chiral derivatizing agent (CDA) 1-fluoro-2,4-dinitrophenyl-5-L-alanine-*amide* (L-FDAA)—Marfey's reagent—which undergoes S_NAr reaction of the 1° amino group. The resulting AA-DAA derivatives are mostly well-separated by reversed-phase HPLC, but some DAA derivatives resist resolution. Here, we report the synthesis and characterization of two CDAs: L-FDTA (**4**) in which the L-alanine-derived auxiliary is replaced by L-tryptophanamide and (S)-FDNE (**3**) where the auxiliary is S-(6-methoxynaphth-2-yl)-1-ethylamine. Side-by-side comparisons of the two reagents were carried out by AA derivatization and reversed-phase HPLC analysis with variables such as organic solvent, additives, and the ionic strength of the mobile phase. L-DTA derivatives of L- and D-AAs were found to show superior HPLC performance and an improvement in resolutions. When incorporated into the mobile phase, the ammonium ion (NH_4^+ , 0–100 mM) showed a dramatic influence on differential retention times [$\Delta t_R = \Delta t_{RD} - \Delta t_{RL}$] of several key AAs. We attributed the effect to π -cation interactions between the indole ring of DTA and the NH_4^+ counterion in the analyte, a hypothesis supported by 1H NMR titrations and DFT calculations.



1. INTRODUCTION

Chiral derivatizing agents (CDAs) have found use for nonempirical analysis of enantiomeric compositions of amino acids (AAs), but perhaps none so widely utilized as the eponymous reagent of Marfey's method.¹ The challenge of assignment of AAs in peptides can be illustrated by the history of enantiomeric analysis of AAs in antitumor cyclic peptides from the Caribbean tunicate *Trididemnum solidum* (Figure 1). The didemnin family of peptides contain less-frequently encountered AAs including D-N-methylleucine, N,O-dimethyltyrosine, and the γ -AA isostatine. Early studies of the structure of didemnin B (**1a**), discovered in 1981 by the Rinehart group and the first marine natural product to enter anticancer clinical trials,² relied on classical methods based on peptide hydrolysis, conversion of the resulting AAs to suitable volatile derivatives, and GC identification of the analytes by comparison with standards. Contemporary HPLC analysis of AA composition and configuration of plitidepsin (dehydrodidemnin B, **1b**, Aplidin)³ from *Aplidium albicans*, and related tamandarins A and B from an unidentified didemnid ascidian,⁴ were achieved efficiently using Marfey's analysis. Plitidepsin (**1b**), now approved for treatment of multiple myeloma,⁵ was also

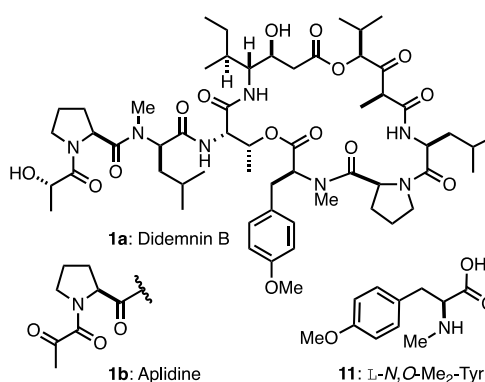


Figure 1. Structures of didemnin B (**1a**), aplidine (**1b**), and L-N,O-dimethyltyrosine (L-N,O-Me₂-Tyr, **11**).

Received: November 22, 2024

Revised: January 24, 2025

Accepted: January 30, 2025

Published: February 20, 2025



discovered to improve clinical outcomes of patients suffering from COVID-19.⁶

The assignment of absolute configuration of α -AAs by Marfey's method relies on reaction of the former with Marfey's reagent, 1-fluoro-2,4-dinitrophenyl-5-L-alaninamide (L-FDAA, **2**), reversed-phase HPLC separation of the resulting diastereomers, and matching the retention times (t_R) against standards prepared in the same way from authentic L- and D-AAs. While Marfey's derivatives of most less-polar L- and D-AAs are well-resolved at long retention times, separations of Marfey's derivatives of polar AAs, such as Ser, Thr, Lys, and Arg, are more challenging. Even among nonpolar AAs, Marfey's method poorly resolves several N^α -Me-AAs, other nonproteinogenic AAs, the classic case of L-Ile and *allo*-D-Ile, while some others, not at all. Variants of Marfey's reagent have been introduced in which the L-alaninamide chiral auxiliary is replaced with L-valinamide,⁷ L-leucinamide,⁸ L-methioninamide,⁹ L-prolinamide, L-phenylglycinamide,⁹ or L-phenylalaninamide.¹⁰ A chiral "diazaspiroketone", derived from (–)-menthone, glycinamide, and 2-fluoro-3,5-dinitrobenzoic acid, has also been assessed in AA analysis.¹¹ These and other Marfey's reagent variants have been extensively reviewed,^{12–14} most recently in 2023 by the comprehensive retrospective by Kijjoo and coauthors.¹⁵

Typically, homologous CDA variants lead to longer and improved retention times, mostly with wider differential retentions on the HPLC column [$\Delta t_R = t_{R(D-AA)} - t_{R(L-AA)}$] due to increased hydrophobicity of the analyte. In most cases, the L-AA-Marfey's derivative elutes before the D-diastereomer. Improvements have also been achieved by altering analytical conditions; for example, the use of LCMS detection with custom mobile phase gradient profiles,¹⁶ alkylammonium phosphate buffers,¹⁰ or replacements of the HPLC C₁₈ stationary phase with shorter-chain (C₃) bonded phase and expansion into the so-called "2D C₃" space.¹⁷

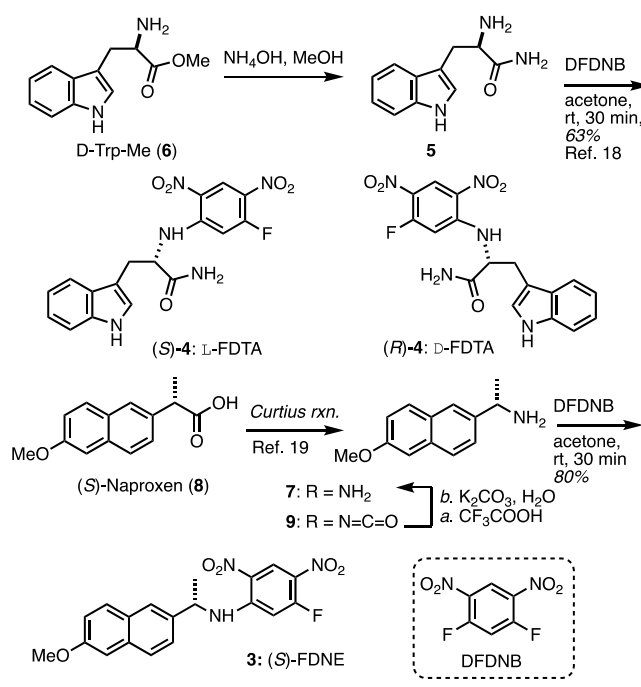
In our investigations of marine-derived peptides, reliable HPLC resolution was required for chiral derivatives of two critical classes of AAs: L- and D-N-Me-Ala and L- and D-Ile from their diastereomeric *allo*-isomers, all notoriously difficult problems with current Marfey-type reagents. We sought to transcend common replacements of the conventional AA-based auxiliaries, designed upon simple empirical leanings toward "more hydrophobic" derivatives, and focus on those containing π -rich aryl and heteroaromatic rings. Our guiding design principle was the introduction of a π -rich donor aromatic ring to the structure of the CDA that would enhance π interactions, alter the dynamics of analyte residency time between mobile and stationary phases during HPLC separation, and improve resolution. It was anticipated prospective replacement of a " π -neutral" phenyl substituent, found in such phenylalaninamide-derived Marfey-type reagents,¹⁰ with a " π -rich ring" would enhance intramolecular π -acid– π -base interactions between the 2,4-DNP, augmented by the usual expected increase in hydrophobic interactions. Additionally, we projected that the inherent fluorescent properties of suitable aryl rings would confer the added advantage of sensitivity through fluorescence detection in critical analyses at the pmole level. Here, we describe the synthesis, characterizations, and deployment of two new CDAs, (S)-**3** and L-**4**, for analysis of enantiomeric compositions of AA derivatives and their scope and limitations for enantiomeric AA analyses.

The syntheses of (S)-**3** and L-**4** were achieved by replacement of L-alaninamide in **2** with one of two chiral amines—S-(6'-methoxynaphth-2'-yl)-1-ethylamine (**5**) and D-tryptophanamide (**6**), respectively. Both reagents were evaluated in side-by-side performance comparisons by derivatization-HPLC analysis of panels of representative AAs and shown to offer complementary advantages over FDAA. Derivatives **4a** of L-FDTA (**4**) with AAs provided superior performance in the most critical cases. A possible mechanism for enhanced HPLC separation is proposed, supported by NMR measurements and computational methods, that invokes π -cation interaction of the NH₄⁺ ion with the aryl rings in HPLC analyte discrimination.

2. RESULTS AND DISCUSSION

Preparation of L-5-fluoro-2,4-dinitrophenyl- N^α -L-tryptophanamide (L-FDTA, S-**4**)¹⁸ was achieved using a variant of Marfey's protocol.¹ D-Tryptophanamide (D-Trp-NH₂, **5**), obtained by ammonolysis of D-Trp methyl ester (**6**, Scheme 1), was

Scheme 1. Synthesis of (S)-FDNE (**3**) and D-FDTA (**4**)

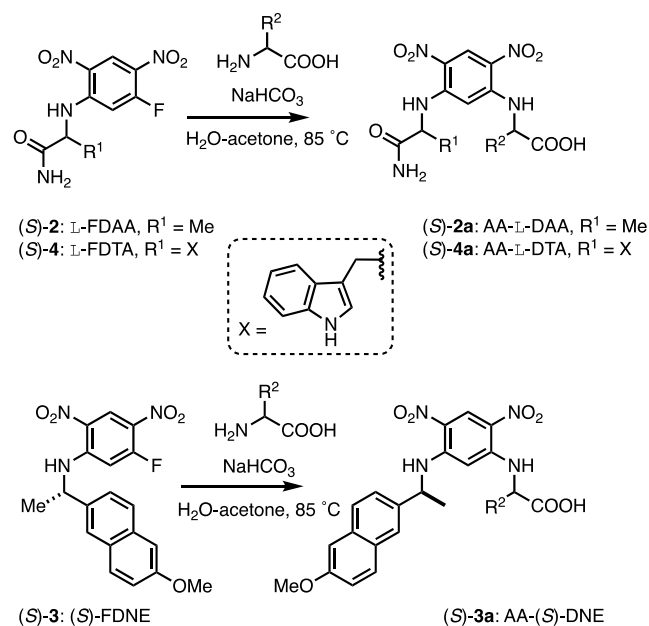


converted to (R)-**4** by reaction with 1,5-difluoro-2,4-dinitrobenzene (DFDNB).¹⁸ In a parallel manner, (S)-(6-methoxynaphth-2-yl)-1-ethylamine (**7**)—conveniently prepared by Curtius reaction of commercial (S)-(+)-naproxen (**8**) to give isocyanate **9**, followed by hydrolysis¹⁹—was reacted with DFDNB to give (S)-(1-fluoro-2,4-dinitrophenyl-naphth-2-yl)-1-ethylamine (FDNE, (S)-**3**).²⁰

The UV–vis spectra of **3** and **4** exhibited long-wavelength absorptions attributed to the dinitrophenyl group identical to that of FDAA (λ_{max} 335 nm, ϵ 14,500); however, the additional chromophores present in **3** and **4** conferred modest improvements in sensitivity of detection due to larger extinction coefficients, ϵ , at shorter λ_{max} (Table S3). Unfortunately, the fluorescent properties of naproxen and Trp were abolished in their derivatives **3a** and **4a** (see Supporting Information) most likely through internal quenching by the 2,4-dinitrophenyl group.

The use of complementary L- and D-Marfey's reagents is useful in cases where only one enantiomer of a particular standard AA is available, say L-. The L-AA-D-Marfey's diastereomer, of course, will have the same retention time as the unavailable and antipodal D-AA-L-Marfey's diastereomer. For the purposes of this study, comparative AA analyses were carried out with different AAs and single enantiomers of CDAs, L-FDAA (2), (S)-FDNE (3), or L-FDTA (4), to give their corresponding diastereomeric derivatives 2a–4a (Scheme 2).

Scheme 2. Derivatization of AAs with L-FDAA (2), L-FDNE (S-3), or L-FDTA (4)



Derivatizations of AAs were carried out by S_NAr substitution with a CDA reagent under conditions slightly modified from Marfey's original protocol (NaHCO₃, H₂O/acetone, 85 °C, 30 min, Scheme 2),¹ which shortened reaction times without compromising efficiency (see Experimental Section).

The retention times t_R of L- and D-AA DTA and DNE derivatives, 4a and 3a, prepared from L-4 and S-3, respectively (Table 1), increased as a function of increased hydrophobicity, in accordance with the mechanism proposed by Harada and co-workers for the separation of AA in the “advanced Marfey's method”.^{21,22} The differences in retention times of the L- and D-AA derivative, Δt_R , were also modulated by hydrophobicity of the aromatic rings.⁸ Differential retention times, Δt_R , of diastereomeric derivatives, 3a, prepared with (S)-3 and a test panel of AAs ((±)-Ala, (±)-Phe, (±)-Glu, (±)-Leu, (±)-Ser, and (±)-Pro) showed poorer resolutions (Table 1) compared to those prepared from L-4 (for conditions of analyses conducted by UHPLC and conventional analytical HPLC, see Experimental Section and table footnotes, below). In contrast, derivatization of AAs with L-4 gave diastereomers with overall increased retention times and improved Δt_R . The order of elution of L-DTA derivatives 4a mostly followed those of L-DAA derivatives 2a (L-AA before D-AA), while—unexpectedly—reversal of retention times was observed for S-DNE derivatives of Leu, Ser, and Pro.

Direct comparative HPLC analysis of an expanded panel of AA derivatives, prepared from Marfey's reagent, L-FDAA (2) and L-FDTA (4), is shown in Tables 3 and 4.²³ The

Table 1. HPLC Analysis^a of L-DNP- and L-DTA-Derivatives (3a and 4a) of Selected (±)-AAs Prepared from (S)-3 and L-4

AA	3a from S-FDNE (3)			4a from L-FDTA (4)		
	retention time, t_R /min		Δt_R^b	retention time, t_R /min		Δt_R^b
	L-	D-	/min	L-	D-	/min
(±)-Ala	7.43	7.43	0.00	8.08	8.86	0.78
(±)-Phe	8.50	8.93	0.43	9.95	10.81	0.86
(±)-Glu	5.53	5.69	0.16	7.49	7.73	0.24
(±)-Leu	8.40	8.14	-0.26	9.98	11.11	1.13
(±)-Ser	5.64	5.53	-0.11	11.08	11.46	0.38
(±)-Pro	7.15	6.95	-0.20	8.21	8.75	0.54

^aHypersil GOLD C₁₈ column, 50 × 2.1 mm (1.9 μm), and a flow rate of 0.500 mL min⁻¹. Elution was conducted with a step gradient of 10% CH₃CN–H₂O–0.1% HCO₂H to 0.3 min to 50% CH₃CN–H₂O/0.1% HCO₂H to 11 min and 100% CH₃CN to 13 min, followed by re-equilibration with 10% CH₃CN–H₂O/0.1% HCO₂H for 2 min; void time, t_0 = 0.53 min. ^b $\Delta t_R = t_{R(D-AA)} - t_{R(L-AA)}$. Negative values indicate reversal of the elution order.

diastereomers were judged to be “resolved” if they showed baseline separation, although partial separations were also considered significant. Similar elution patterns were observed for both the L-DAA and L-DTA derivatives of most of the neutral AAs; for example, the L-AA derivative eluted before the D-AA isomer. Under the same conditions (see footnote of Table 2), neither reagent resolved (±)-Asp, while only reaction with L-4, followed by HPLC, allowed resolution of both (±)-citrulline and (±)-Ser.

Major differences were observed for DTA derivatives of polar AAs (±)-Glu and (±)-N-Me-Asp: D-AA derivatives eluted before their L-diastereomers. For the basic AAs, (±)-Lys, (±)-Orn, and (±)-His, with two reactive amino groups (α -NH₂, ω -NH₂ groups, or imidazole), both mono- and diderivatives were obtained. Pairs of mono- α -N and di- N,N' -L-DAA derivatives of all three basic AAs were well-resolved, but in contrast, the corresponding L-DTA derivatives showed poor resolution (Δt_R) for L- and D-AAs, despite increased retention times. The L-DTA derivatives of (±)-Tyr, which has two nucleophilic groups (phenoxy and α -NH₂), gave a similar result. The latter observations imply a change in the mechanism of separation for the AA derivatives. Notably, the L-DAA derivatives of the enantiomers of Ser, *iso*-Ser, *N*-Me-Ala, and citrulline (Table 2) failed to resolve, but were well-separated as their L-DTA derivatives (Table 3, see also S2). For example, L-DTA-Ser, L-DTA-*iso*-Ser, L-DTA-*N*-Me-Ala, and L-DTA-citrulline showed differential separations of $\Delta t_R = 0.50, 0.37, 0.55,$ and -0.38 min, respectively. Some L-DTA derivatives (e.g., Asn and Lys) gave poor or no resolution which comes as no surprise as no one CDA can be expected to optimally resolve all AA derivatives across a range of polarities. Interestingly, mono- α -L-DTA-Orn showed no separation (Table 3), but di- α,γ -L-DTA-Orn diastereomers were resolved ($\Delta t_R = 0.21$ min).

A perennial challenge in AA analysis using modified Mosher's methods has been efficient separation of derivatives of Ile and D-*allo*-Ile. While Ile and L-*allo*-Ile are readily separated (e.g., using Capon's “2D C₃” variant of Marfey's method paired with DAA derivatives),¹⁷ the resolution of L-Ile and D-*allo*-Ile has always been problematic. In natural product peptides, D-*allo*-Ile arises from L-Ile residues by α -epimerization

Table 2. Analyses of Marfey's (L-DAA) Derivatives of (\pm)-AAs^a

AA	elution order	retention time, min		Δt^b , min	resolved?	α^c
		L-AA	D-AA			
Ala	L → D	5.20	7.38	2.18	Y	1.42
norvaline	L → D	10.28	13.78	3.50	Y	1.34
Val	L → D	9.73	13.25	3.52	Y	1.36
Leu	L → D	13.25	16.55	3.30	Y	1.25
Ile	L → D	12.67	16.18	3.51	Y	1.28
Met	L → D	8.98	12.30	3.32	Y	1.37
Phe	L → D	13.28	16.16	2.88	Y	1.22
Tyr (di-N,O)	L → D	18.97	21.45	2.48	Y	1.13
Pro	L → D	5.23	6.10	0.87	Y	1.17
Ser	L → D	3.02	3.02	0.00	N	1.00
allo-Thr	L → D	3.57	4.40	0.83	Y	1.23
Asn	^d	2.72	2.72	0.00	N	1.00
Glu	L → D	4.46	5.57	1.11	Y	1.25
Asp	L → D	3.57	4.55	0.98	Y	1.27
Lys (mono- α)	L → D	2.11	3.21	1.10	Y	1.52
Lys (di- α,ϵ)	L → D	19.19	21.36	2.17	Y	1.11
Orn (mono- α)	D → L	2.26	1.76	-0.50	N	1.28
Orn (di- α,δ)	D → L	16.93	15.25	-1.68	Y	1.11
His (mono- α)	D → L	1.72	1.50	-0.22	N	1.15
His (di- α,δ)	L → D	9.48	11.60	2.12	Y	1.22
Arg	L → D	1.76	2.07	0.31	N	1.18
Cit	^d	4.15	4.15	0.00	N	1.00
N-Me-Ala	^d	8.39	8.39	0.00	N	1.00
N-Me-Asp	D → L	3.49	4.29	0.80	Y	1.23
iso-Ser	^d	3.82	3.82	0.00	N	1.00
N,O-Me ₂ -Tyr ^e	L → D	18.50	19.04	0.54	Y	1.03

^aUHPLC conditions: Hypersil GOLD C₁₈ column, 50 × 2.1 mm (1.9 μ particle), and a flow rate of 0.50 mL min⁻¹. Elution was completed with a linear gradient of 15%–45% CH₃CN–H₂O/0.1% HCOOH for 25 min, followed by 100% CH₃CN for 2 min and re-equilibration with 15% CH₃CN–H₂O/0.1% HCOOH for 3 min. ^b $\Delta t_R = t_{R(D-AA)} - t_{R(L-AA)}$. ^c $\alpha = (t_{R(A)} - t_0)/(t_{R(B)} - t_0)$, where t_0 is void time and A and B are the slower and faster eluting components, respectively. For definitions of other parameters, see footnotes of Table 1. ^dCo-eluted diastereomers. ^eN-Methyl-O-methyl tyrosine.

(epimerase-mediated) in the cognate NRPS assembly line. We were pleased to observe excellent separation of the DTA derivatives of L-Ile and D-*allo*-Ile (Table 3) ($\Delta t_R = 1.03$ min), an improvement over the corresponding DAA diastereomers (Table 4, $\Delta t_R = 0.16$ min).²⁴

Resolution of N ^{α} -methyl AA derivatives can also be challenging. L- and D-N-Me-Ala DAA derivatives (2a, Table 3) failed to separate under conditions where the corresponding DTA derivatives, 4a, were resolved ($\Delta t_R = 1.03$ min). L- and D-N-Me-Asp DTA and DAA derivatives (4a and 2a) were both cleanly resolved (Tables 3 and 4). Notably, the L- and D-N-Me-Asp-DTA 4a were well-separated ($t_R = 11.67$ and 10.51 min, $\Delta t_R = -1.16$ min, respectively; note reversal of elution order), albeit at retention times longer than their DAA counterparts, 2a ($t_R = 3.49$ and 4.29 min, $\Delta t_R = 0.80$ min).

Further examination of the separation characteristics of those critical AAs with $\Delta t_R \leq 1.00$ min was carried out by testing the effect of ammonium acetate in the HPLC mobile phase (NH₄OAc, 20 mM) on the elution behavior of L-DTA-derivatives. Some literature variants of Marfey's method have employed salt in the mobile phase: either Et₃NH⁺ phosphate or volatile NH₄OAc. In the present work, aqueous CH₃CN gradients (0.1% TFA or HCO₂H), without salt buffer, effected little or no separations of some AA-L-DAA derivatives (2a, e.g., AA = (\pm)-Ser, (\pm)-*iso*-Ser, and (\pm)-citrulline, Tables 3 and 4) in contrast to the literature results for (\pm)-Ser which resolved under similar elution conditions.¹⁰ The latter observation

suggests some dependency of separation upon the stationary phase, e.g., column particle homogeneity, differences in proprietary column composition, or simply age-related column degradation.

Improved resolution was observed for most of the AA L-DTA derivatives in the presence of NH₄OAc in the mobile phase (Table 4); these included (\pm)-Lys, (\pm)-Orn, (\pm)-His, (\pm)-Asp, and (\pm)-N-Me-Ala. The L-DAA-derivatives of AA with different charged side chains (\pm)-citrulline (neutral) and (\pm)-Arg (positive) failed to separate and coeluted as one peak. The largest improvement in separation—defined as $\Delta\Delta t_R$, the difference of absolute values of Δt_R in the presence and absence of NH₄OAc, respectively—occurred with (\pm)-Arg and (\pm)-Lys, which failed to resolve under the former conditions (Table 3) but were successfully resolved as DTA derivatives (Table 5). The diastereomers of (\pm)-Arg-L-DTA showed improved separation ($\Delta\Delta t_R = -0.62$ min), while the N ^{α,ϵ} -double-derivative (\pm)-Lys-[L-DTA]₂ separated with the largest difference in retention times ($\Delta\Delta t = 10.11$ min) under the latter conditions (Table 5).

The origin of the dramatic effect of NH₄OAc upon retention times, where the mobile phase is set to approximately pH ~ 7 ,²⁵ appears to be related to two properties: the completely ionized RCO₂⁻ group of the AA and the presence of the indole heterocycle. Contrary to presumptions of the dominance of H-bonding interactions between stationary and mobile phases in HPLC separations, the key interactions of Marfey's derivatives,

Table 3. HPLC Analyses^a of L-DTA Derivatives of (±)-AAs

AA		DTA			
		<i>t_R</i> , min			
		L	D	Δt_R^b	α^b
Ala	L → D	13.08	15.52	2.44	1.19
Nva ^c	L → D	16.79	20.26	3.47	1.21
Val	L → D	16.22	19.85	3.63	1.22
Leu	L → D	18.85	22.36	3.51	1.19
Ile	L → D	18.40	22.06	3.66	1.20
Met	L → D	15.75	18.88	3.13	1.20
Phe	L → D	18.83	21.60	2.77	1.15
<i>N,O</i> -Me ₂ -Tyr (11)	L → D	25.87	26.10	0.23	1.01
Pro	L → D	13.57	15.28	1.71	1.13
Ser	L → D	10.43	10.93	0.50	1.05
<i>allo</i> -Thr	L → D	10.98	12.24	1.26	1.11
Asn	^d	9.73	9.73	0.00	1.00
Glu	D → L	12.82	11.92	-0.90	1.08
Asp	L → D	10.79	11.76	0.97	1.09
Lys (mono- α)	^d	9.91	9.91	0.00	1.00
Lys (di-a,e)	^d	24.02	24.02	0.00	1.00
Orn (mono- α)	^d	8.93	8.93	0.00	1.00
Orn (di-a,d)	L → D	22.30	22.51	0.21	1.01
His (mono- α)	D → L	7.53	6.34	-1.19	1.19
His (di)	L → D	19.65	20.37	0.72	1.04
Arg	L → D	8.12	8.74	0.62	1.08
Cit ^e	D → L	10.93	11.31	0.38	1.03
<i>N</i> -Me-Ala	L → D	19.40	19.95	0.55	1.03
<i>N</i> -Me-Asp	D → L	11.67	10.51	-1.16	1.11
<i>iso</i> -Ser ^f	L → D	16.67	17.04	0.37	1.02
Ile ^g	L → D	34.41			
<i>allo</i> -Ile ^g	L → D	33.38			

^aConditions: Reversed-phase C₁₈ column, 50 × 2.1 mm (1.9 μ m), flow rate 0.50 mL min⁻¹; elution completed with a linear gradient of 15–45% CH₃CN/H₂O-0.1% HCOOH for 25 min, followed by 100% CH₃CN for 2 min and re-equilibration with 15% CH₃CN/H₂O-0.1% HCOOH for 3 min before the next measurement; void time *t*₀ = 0.53 min. ^bFor definition of parameters, see the footnotes of Tables 1 and 2. ^cNorvaline. ^dCo-elution. ^eCitrulline. ^fIso-serine (3-amino-2-hydroxypropanoic acid). ^gConditions: Agilent Zorbax SB-Aq column, 4.6 × 250 mm (5 μ m), stepped gradient, initial conditions 30–40% CH₃CN/H₂O/20 mM NH₄OAc-0.1% trifluoroacetic acid (TFA), 40 min; 40–50% CH₃CN/H₂O/20 mM NH₄OAc-0.1% TFA, flow rate 0.7 mL min⁻¹.

2a–4a with reversed-phase stationary phases (e.g., C₁₈), are hydrophobic in nature. It has been proposed that a combination of intramolecular H bonding and non-H bonding orders the structures of diastereomeric analytes, AA-DAA, creating a “more compact L–L diastereomer” compared to L–D.²⁶ An increase in hydrophobicity of the analyte molecule (supported by analysis of CPK models) is proposed and evidenced by comparative analysis of retention times of D- and L-AAs.²⁵ Conversely, Harada and coauthors argue a mechanism (supported by NOE measurements) independent of hydrogen bonding.⁸ Either way, AA derivatives 4a also show enhanced hydrophobicity (increased *t_R*) through a compaction of the analyte structure but with a secondary element of control absent from other Marfey-type reagents: π – π and cation– π interactions (see below) with the heterocyclic ring in Trp-NH₂ that fine-tune molecular discrimination of analytes 4a (see Scheme 1).

Generally, the longer retention times observed during reversed-phase HPLC in the presence of NH₄⁺ (Table 5) imply more hydrophobic mobile species than those in the absence of NH₄⁺. We attribute the improved resolutions of 4a to discrete intramolecular π -base properties of the electron-rich indole ring of Trp-NH₂. The latter may include intramolecular π – π interactions with aromatic analytes or attractive π –cation interactions²⁷ induced by Na⁺, R₃NH⁺, or NH₄⁺ counterions in the HPLC mobile phase, carboxylate ion pair, or a combination of both.

¹H NMR data supports the conformation presented in structure 10 (Figure 2). The chemical shift of H-5 in the dinitrophenyl ring is unusually high (δ 5.6 ppm, cf. H-2, δ 9.8), which is explained by diamagnetic shielding induced by the indole ring current in a conformation that is folded (compacted). We briefly investigated the conformation of the L-DTA derivative of L-Ala (10, Figure 2) by geometry-minimized structures (MMFF) further refined by DFT quantum mechanical calculations (Spartan '14, EDF2 6-31G* 6-31G(D)). The lowest-energy conformers of neutral 10 (Figure 2b depicts the most stable conformer) adopt a conformation that stacks the electron-poor DNP ring above the electron-rich benzenoid ring of indole. Although both aromatic rings are *syn* to each other, their planes are displaced by an angle of approximately 33°. Importantly, the constraints imposed by attractive electrostatic dipole–dipole interactions and torsional angles actively cooperate to compact the structure in a way that disposes the side chain of the Ala side chain to the exterior. Introduction of the NH₄⁺ counterion is expected to build stabilization through a π –cation interaction, Figure 2a; however, accurate calculations of this entity would, of necessity, include solvation of both charged groups, with appropriate parameterization, requisites that are beyond the scope of this report. Nevertheless, a detailed understanding of this phenomenon may inform design of new optimized Marfey's-type reagents based on non-natural AAs and is currently a subject of exploration in our laboratory.²⁸

As reported earlier by Fujii and co-workers,⁸ several lines of evidence suggest that the diastereomeric discrimination between Marfey's derivatives has less to do with hydrogen bonding in solvent–analyte interaction and more with hydrophobicity of analyte–stationary phase association.⁸ We hypothesize that a pronounced intramolecular π –cation interaction between the NH₄⁺ counterion and the electron-rich indole ring presents a more compact, hydrophobic mobile species to the stationary phase that enhances molecular discrimination between D- and L-AAs derivatives. In both the neutral carboxylic acid (for simplicity we refer to this structure as 10•H, Figure 2, minimized geometry, MMFF, and DFT-calculated energy) and the corresponding ammonium salt as 10•NH₄⁺. Strong dipole or charge interactions, respectively, between the carboxyl terminus and the electron-rich indole ring shield the polar groups within two hydrophobic “walls” comprising the two aryl ring systems—indole and 2,4-dinitrophenyl ring (DNP). The deviation in conformation leads to compaction of the analyte molecular structure in high-dielectric aqueous HPLC mobile species. The DFT-calculated molecular geometry of the ammonium salt 10•NH₄⁺ (ω B97X-D, 6-31G*, polar solvent) shows an even tighter association of the 2,4-dinitrophenyl ring (DNP) and indole rings; the two planes deviate only ~16° from parallel; (see Supporting Information). In the NH₄⁺ salts of traditional Marfey's derivatives obtained with FDAA, such a π –cation interaction

Table 4. HPLC Analyses of Critical L-DAA-AAs and L-DTA-AAs, 2a and 4a in the Presence of NH₄OAc^a

AA	L-DAA				L-DTA			
	<i>t_R</i> , min		Δt_{R}^b	α^c	<i>t_R</i> , min		Δt_{R}^b	α^c
L	D	L			D			
<i>N,O</i> -Me ₂ -Tyr (11)	45.54	46.38	0.83	1.02	37.76	39.28	1.53	1.05
Ser	29.67	29.99	0.32	1.01	21.39	22.36	0.97	1.06
Asn	28.35	28.35	0.00	1.00	20.74	21.85	1.11	1.07
Glu	31.21	31.51	0.30	1.01	19.67	20.08	0.41	1.03
Lys (mono- α)	25.86	24.38	-1.48	1.08	22.04	22.04	0.00	1.00
Lys (di- α,ϵ)	26.33	26.33	0.00	1.00	24.88	34.99	10.11	1.52
Orn (mono- α)	25.48	25.48	0.00	1.00	24.06	24.06	0.00	1.00
Orn (di- α,δ)	41.98	41.98	0.00	1.00	33.81	32.98	-0.83	1.03
His (mono- α)	24.93	23.44	-1.49	1.08	22.34	21.80	-0.54	1.03
His (di- α,δ)	34.34	34.69	0.35	1.01	32.42	32.99	0.57	1.02
Arg	26.61	25.17	-1.44	1.07	23.14	23.14	0.00	1.00
Cit ^d	29.23	28.12	-1.11	1.05	22.02	22.02	0.00	1.00
<i>N</i> -Me-Ala	34.32	34.88	0.57	1.02	24.26	25.53	1.28	1.07
<i>N</i> -Me-Asp	30.43	29.68	-0.74	1.03	18.99	18.54	-0.45	1.03
<i>iso</i> -Ser ^e	29.70	29.98	0.28	1.01	23.28	23.28	0.00	1.00
<i>allo</i> -Ile	39.33	42.56	3.23	1.10	26.62	30.01	3.39	1.16
Ile	39.43	42.58	3.16	1.09	26.52	29.85	3.33	1.16

^aConditions: Reversed-phase C₁₈ column, 250 × 4.6 mm (5 μ m), flow rate 0.70 mL min⁻¹; elution completed with a linear gradient of 15–65% CH₃CN/0.1 M NH₄OAc–H₂O–0.1% TFA for 40 min, followed by 100% CH₃CN for 5 min; void time *t*₀ = 5.31 min. ^b $\Delta t = t_{\text{R}}(\text{D-AA}) - t_{\text{R}}(\text{L-AA})$. ^c $\alpha = [t_{\text{R}}(\text{B}) - t_0]/[t_{\text{R}}(\text{A}) - t_0]$, where A and B are the faster and slower eluting components, respectively. ^dCitrulline. ^e(\pm)-Amino-2-hydroxypropanoic acid.

Table 5. HPLC Analyses of Differential Retention Times (*t_R*, Δt_{R} , and $\Delta\Delta t_{\text{R}}$) of Critical L-DTA Derivatives, 4a, of AAs in the Presence of NH₄OAc

AA ^a	<i>t_R</i> , min		Δt_{R}^b , min	$\Delta\Delta t_{\text{R}}^c$, min	resolved?
	L-AA	D-AA			
<i>N,O</i> -Me ₂ -Tyr (11)	37.76	39.28	1.53	1.3	Y
Ser	21.39	22.36	0.97	0.47	Y
Asn	20.74	21.85	1.11	1.11	Y
Glu	20.08	19.67	-0.41	-0.49	Y
Lys (mono- α)	22.04	22.04	0.00	0	N
Lys (di- α,ϵ)	24.88	34.99	10.11	10.11	Y
Orn (mono- α)	24.06	24.06	0.00	0	N
Orn (di- α,δ)	33.81	32.98	-0.83	0.62	Y
His (mono- α)	22.34	21.80	-0.54	-0.65	Y
His (di- α,δ)	32.42	32.99	0.57	-0.15	Y
Arg	23.14	23.14	0.00	-0.62	N
Cit	22.02	22.02	0.00	-0.38	N
<i>N</i> -Me-Ala	24.26	25.53	1.28	0.73	Y
<i>N</i> -Me-Asp	18.99	18.54	-0.45	-0.71	Y
<i>iso</i> -Ser	23.28	23.28	0.00	-0.37	N
<i>allo</i> -Ile	26.62	30.01	3.39	-0.3	Y
Ile	26.52	29.85	3.33	-0.19	Y

^aConditions: Luna C₁₈ column (250 × 4.6 mm, 5 μ m) and a flow rate of 0.70 mL min⁻¹. Elution was carried out with a linear gradient of 15–65% CH₃CN–0.10 M NH₄OAc–0.1% TFA for 40 min, followed by 100% CH₃CN for 5 min. ^b $\Delta t = t_{\text{R}}(\text{D-AA}) - t_{\text{R}}(\text{L-AA})$. Negative values indicate reversal of the elution order. ^c $\Delta\Delta t_{\text{R}} = |\Delta t_{\text{R}}(\text{Table 4})| - |\Delta t_{\text{R}}(\text{Table 3})|$. Negative values indicate poorer resolution with DTA derivatives.

would, of course, be unlikely as the only delocalized π -system available is the electron-deficient 2,4-DNP ring; here, an “ammonium ion effect” would be prohibited. This intriguing

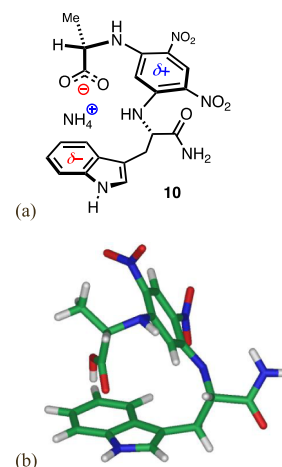


Figure 2. π -cation interactions in the L-DTA-derivative of L-alanine (10. See Scheme 2). (a) Representational model of the NH₄⁺ salt of 10. (b) Calculated model (DFT) of neutral 10•H (Spartan '14, EDF2 6-31G* 6-31G) (D). See Supporting Information for the DFT z file of calculated structure 10•NH₄⁺ (ω B97X-D, 6-31G*, polar solvent).

property is the subject of ongoing investigation in our laboratory.

Evidence for the π -cation interaction was obtained from ¹H NMR measurements of 10 with titration by ammonium acetate (600 MHz, DMSO-*d*₆, NH₄OAc, Figure 3). In the absence of NH₄OAc, the downfield region of the ¹H NMR spectrum (δ 6–9 ppm) was populated only by aromatic signals of the indole and dinitrophenyl rings and the NH signal (δ 7.41, br s). Upon addition of NH₄OAc (0.1–1.0 equiv), a new 1:1:1 triplet signal grew in (δ 7.08, *t*, ¹*J*_{IH–14N} = 47.6 Hz), corresponding to the NH₄⁺ ion signal, which increased in intensity up to 1.0 equiv of NH₄OAc. Observation of discrete one-bond ¹H–¹⁴N heteronuclear coupling constants to the ¹⁴N nucleus (spin *I* = 1) implied the presence of NH₄⁺ in the ion

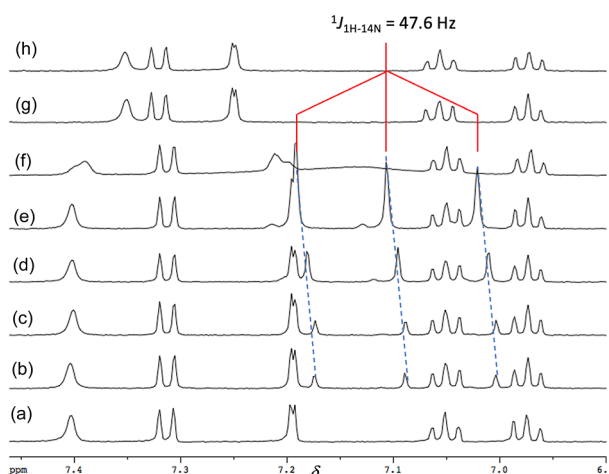
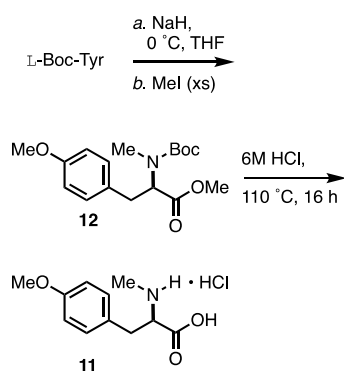


Figure 3. ^1H NMR titration of *L*-Ala-*L*-DTA (**10**, 600 MHz, $\text{DMSO-}d_6$) (a), no NH_4OAc (b), 0.1% TFA and 0.1 equiv. NH_4OAc (c), 0.2 equiv. (d), 0.5 equiv. (e), 1.0 equiv. (f), 2.0 equiv. (g), 5.0 equiv. (h) 10.0 equiv. Dashed lines and ^1H NMR “splitting tree” indicate a discrete NH_4^+ $^1\text{H-}^{14}\text{N}$ couplet (1:1:1, $^1J_{\text{NC}} = 47.6$ Hz).

pair $10 \bullet \text{NH}_4^+$ (here, **10** is in its conjugate base form) within a relatively symmetrical electronic environment and in a slow exchange regime. Addition of excess NH_4OAc (2.0–10.0 equiv) resulted in progressive broadening of the NH_4^+ signal, until it merged completely into the baseline. Other dramatic changes in the indole ^1H chemical shifts were observed. This is consistent with disruption of the discrete stoichiometric species (1:1 $\text{NH}_4^+:\text{10}$) undergoing rapid intermolecular exchange with NH_4^+ outside of the first sphere of coordination with concomitant signal broadening.

Finally, we revisited the historical antitumor cyclodepsipeptide, didemnin B (**1a**), and applied **4** to the analysis of the constituent AA residues. Standard *L*-*N,O*- Me_2 -Tyr hydrochloride (**11**) was synthesized by *N*-methylation of *N*-Boc-Tyr (NaH, excess MeI, THF, Scheme 3) to give ester **12**

Scheme 3. Synthesis of *L*-*N,O*- Me_2 -Tyr



followed by acid hydrolysis (6 M HCl, 110 °C, see Experimental Section) to deliver **11**. Hydrolysis of **1b** (6 M HCl, 110 °C, 16 h), followed by derivatization of the resultant AA mixture with *L*-**4** and *D*-**4** and LCMS analysis of the products **4a**, revealed diastereomers arising from *L*-Pro, *N*-*M*-*D*-Leu, and, *N,O*- Me_2 -*L*-Tyr, consistent with prior analyses,⁴ but with improved Δt_{R} of *L*-**11**-DTA versus *L*-**11**-DAA (Δt_{R} 1.53 and 0.83 min, respectively. See Table 4), albeit slightly less in the presence of NH_4OAc ($\Delta \Delta t_{\text{R}} = 1.3$, Table 5).

3. CONCLUSIONS

Two new CDAs, both Marfey-type reagents, **3** and **4** for derivatization and chiral analysis of *L*- and *D*-AAs, were designed and synthesized from optically pure amines, (*S*)-**5** (derived from *S*-naproxen) and *L*-Trp, respectively. Evaluation of HPLC analysis of AA derivatives **3a** and **4a** of the two CDAs, reagent **3** was outperformed by the tryptophanamide-derived reagent **4** in side-by-side comparisons. The new reagent FDTA (**4**) was also shown to be superior to Marfey's reagent (**2**) for HPLC analysis of the corresponding derivatives of several polar proteinogenic AAs and key nonproteinogenic AAs, including *iso*-Ser and *N*^α-methylated AAs including *N*-Me-Ala and *N,O*-Tyr. A working hypothesis was proposed for the basis of the diastereomeric discrimination of DTA derivatives on HPLC. A notable ‘ NH_4^+ cation effect’ of DTA derivatives was observed and supported by ^1H NMR titration of **10** with NH_4OAc (Figure 3, **4a**, $R^2 = \text{Me}$), which invokes intramolecular π -cation interaction of the NH_4^+ counterion between the electron-poor and electron-rich aromatic 2,4-dinitrophenyl and Trp indole ring systems, respectively.

4. EXPERIMENTAL SECTION

4.1. General Experimental Procedures. 1,5-Difluoro-2,4-dinitrobenzene and *L*- and *D*-AAs were purchased from Sigma-Aldrich (St. Louis, MO). FDAA, *L*-tryptophan, and HCOOH were purchased from Thermo Fisher Scientific (Waltham, MA). Ammonium hydroxide and TFA, AR grade, were purchased from EMD Millipore (Chicago, IL). Ammonium acetate (AR, >99%) was purchased from Macron Fine Chemicals (Avantor, Center Valley, PA). All other solvents were of HPLC or LCMS grade and purchased from Thermo Fisher Scientific (Waltham, MA). Optical rotations were measured on a JASCO P-2000 at the D-double emission line of Na. Analytical HPLC was carried out on an integrated JASCO system consisting of dual-pumps (PU-2086 Plus), a dynamic mixer (MX-2080-32), and a UV-vis detector (UV-2075). UV-vis spectra were measured on a JASCO V-630 spectrometer using a quartz cell (1 mm path length). FTIR spectra were collected on thin film samples using a JASCO FTIR-4100 fitted with an ATR accessory (ZnSe plate). 1D-NMR and inverse-detected 2D NMR spectra were measured on a Bruker Avance III (600 MHz) NMR spectrometer with a 1.7 mm $^1\text{H}\{^{13}\text{C}\}\{^{15}\text{N}\}$ microcryoprobe. Other NMR spectra were measured on a JEOL ECA 500 spectrometer equipped with a 5 mm $^1\text{H}\{^{13}\text{C}\}$ room temperature probe at 500 MHz. ^{13}C NMR spectra were measured using a Varian VX 500 NMR spectrometer equipped with a 5 mm Xsens $^{13}\text{C}\{^1\text{H}\}$ cryoprobe at 125 MHz. NMR spectra are referenced to residual solvent signals (CDCl_3 , δ_{H} 7.26, δ_{C} 77.00 ppm; $\text{DMSO-}d_6$, δ_{H} 2.50, δ_{C} 39.52 ppm; acetone- d_6 , δ_{H} 2.05, δ_{C} 205.87 ppm). High-resolution ESITOF analyses were carried out on an Agilent 6350 TOF MS coupled to an Agilent 1200 HPLC at the Small Molecule MS Facility (UCSD). Low-resolution MS measurements were made using a ThermoFisher Surveyor UHPLC coupled to a UV-vis detector (PDA) and an MSD single-quadrupole detector.

4.2. Animal Material. *T. solidum* Van Name, 1902, was collected from Little San Salvador, Bahamas, in 1999 by scuba at a depth of −20 m and stored at −20 °C until required. A voucher sample is archived at UC San Diego.

4.3. Extraction and Isolation of Didemnin B (1a) from *T. solidum*. Didemnin B (**1a**) was isolated from extracts of a frozen sample of *T. solidum* that had been stored at −20 °C as previously described.²⁹

4.4. *S*-(+)-Naproxen. Commercial “over-the-counter” Naproxen Sodium tablets (CVS brand, 250 mg, ~50 count, 13 g) were ground to a fine powder and dispersed/dissolved in water (~500 mL). The mixture was made basic (NaOH, pH ~ 10) and stirred briefly, and the suspension filtered (Whatman no. 1 paper) to remove excipients. The filtrate was cooled to 0 °C and carefully acidified (6 M HCl), and the precipitate of *S*-(+)-Naproxen filtered and dried under reduced

pressure in a desiccator over KOH. The crude solid was ground in a mortar and pestle to a fine colorless powder [$[\alpha]_D^{20} +65$ (CHCl₃), lit.³⁰ +66 (CHCl₃)]. ¹H NMR matched literature values.³¹ S-(+)-Naproxen was used in the next step without further purification.

4.5. (6-Methoxynaphth-2-yl)-1-ethylamine (6). S-(+)-Naproxen (0.531 g, 2.30 mmol) was subject to Curtius rearrangement according to the method of Mutschler and co-workers,¹⁹ to give (S)-2-(1-isocyanatoethyl)-6-methoxynaphthalene (5a) as a colorless solid (0.319 g, 61%). Conversion of 5a to 5 was completed by hydrolysis (CF₃COOH, reflux, followed by K₂CO₃, H₂O, rt), and extractive workup (EtOAc) gave the optically pure amine (S)-1-(6-methoxynaphth-2-yl)-1-ethylamine, (S)-5³² which was carried forward to the next reaction.

4.6. (S)-5-Fluoro-N-(1-(6-methoxynaphth-2-yl)ethyl)-2,4-dinitroaniline (3).¹ A solution of (S)-5 (44.5 mg, 0.221 mmol) in 1 N NaOH (0.2 mL) and acetone (3 mL) was treated with anhydrous MgSO₄ (0.5 mg) with continuous stirring over for 15 min. The mixture was filtered and the residue washed with a little cold acetone, and the filtrate and washings combined with a solution of 1,3-difluoro-2,4-dinitrobenzene (45.0 mg, 0.221 mmol): *Caution! Acutely toxic, skin irritant!* in acetone (2.0 mL) and stirred at 23 °C for 45 min during which the color changed to a bright orange. H₂O was added to precipitate the crude product, and the entire suspension passed through a short column of Celite. The column was washed with a little H₂O, and the product was dissolved and eluted with acetone. After removal of the volatiles and drying under high vacuum, (S)-3 was obtained as a bright-yellow-orange solid (68.1 mg, 80%). (S)-3; $[\alpha]_D^{24.2} +200$ (c 0.22, CH₃CN); UV (MeOH) λ_{max} 232 nm (ϵ log 4.75), 262 (4.05), 334 (4.10); FTIR (ATR, ZnSe plate) ν 3357, 2936, 1630, 1606, 1582, 1542, 1521, 1484, 1422, 1366, 1330, 1287, 1267, 1177, 1103, 1055, 1029, 918, 855, 833, 740, and 711. ¹H NMR (600 MHz, acetone-*d*₆): δ 9.01 (2H, d, 7.8), 7.97 (1H, s), 7.85 (1H, d, 8.4), 7.78 (1H, d, 8.4), 7.61 (1H, dd, 8.4, 1.8), 7.30 (1H, d, 2.4), 7.15 (1H, dd, 9.0, 2.4), 6.89 (1H, d, 14.4), 5.21 (1H, m), 3.91 (3H, s), 1.82 (3H, d, 6.6). ¹³C{¹H} NMR (125 MHz, DMSO-*d*₆): δ (ppm): 159.9, 157.8, 157.4, 148.3 {148.2}, 137.3, 133.8, 129.4, 128.3, 127.6, 127.4, 124.9, 124.5, 119.0, 105.9, 102.7, 102.5, 55.3, 52.9, and 23.2. HRMS(ESI-TOF) m/z [M + H]⁺ calcd for C₁₉H₁₆N₃O₃FNa 408.0972; found 408.0968.

4.7. L-5-Fluoro-2,4-dinitrophenyl-N^α-L-tryptophanamide (L-FDTA, 4). Reagent 4 was prepared from L-tryptophan as previously described.¹⁸

4.8. Analytical Chromatography. LC APCI-MS and ESI-MS spectra were obtained on a Thermo Fisher UHPLC, coupled to a Thermo Fisher MSD quadrupole detector. Separations were carried out using a Hypersil GOLD C₁₈ column, 50 × 2.1 mm (1.9 μm particle), and a flow rate of 0.500 mL min⁻¹. Elution was conducted with a linear gradient of 15% to 45% CH₃CN/H₂O-0.1% HCOOH for 25 min, followed by 100% CH₃CN for 2 min and re-equilibration with 15% CH₃CN/H₂O-0.1% HCOOH for 3 min before the next measurement. Analytical HPLC measurements were carried out using a Luna C₁₈ column (250 mm × 4.60 mm, particle size 5 μm) and 0.700 mL flow rate with UV detection (λ = 335 nm). Elution was completed with a linear gradient of 15% to 65% CH₃CN/H₂O-0.1% TFA or CH₃CN/0.1 M NH₄OAc-0.1% TFA for 40 min followed by a 5 min wash with 100% CH₃CN and re-equilibration with 15% CH₃CN/H₂O-0.1% TFA or CH₃CN/0.1 M NH₄OAc, 0.1% TFA, respectively. See also the conditions listed in the table footnotes.

4.9. Derivatization of L-, D-, and DL-AAs by 2–4. The following is a representation of AA derivation by 2–4. To a 3.8 mL vial equipped with a magnetic stir bar was added an aqueous solution of DL-AA (10 mM, 250 μL, 2.5 μmol), followed by a solution of L-FDTA (4) or S-FDNE (3) or L-FDAA (2) in acetone (1% w/v, 140 μL, 3.6 μmol), aqueous NaHCO₃ (1 M, 20 μL, 20 μmol), and acetone (200 μL). The mixtures were stirred at 85 °C for 30 min, cooled to room temperature, and neutralized with 1 M HCl (20 μmol). For LC–MS analysis, aliquots of the derivatized AAs (20 μL) were diluted with MeOH (80 μL) and centrifuged, and an aliquot of each solution (10 μL) analyzed by HPLC under the conditions described in the footnotes of Tables 3–5. Retention times and peak areas were

determined by using native software. Standard AAs, racemic (±)- or L- and D-AAs, were prepared and analyzed in the same manner. See Tables 3–5.

4.10. L-N,O-Dimethyltyrosine (11). A stirred solution of L-N-Boc-Tyr (2.00 g, 7.1 mmol) in THF (40 mL) was cooled to 0 °C. NaH (60% w/w dispersion in mineral oil, 4.0 equiv) was added in one portion, and the solution was stirred for an additional 15 min at 0 °C. Iodomethane (0.574 g, 14.36 mmol, 5.0 equiv. *Caution! Acute toxicity, inhalation hazard!*) was added slowly, and the mixture allowed to warm to 23 °C over 20 h. The solution was carefully quenched by dropwise addition of H₂O and diluted with additional H₂O (50 mL) before extraction with EtOAc (×3). The combined organic extracts were washed with brine, dried over MgSO₄, and concentrated to a yellow oil which was purified by flash chromatography (SiO₂, 3:1 hexanes-Et₂O to 100% Et₂O) and gave N-Boc-11 as a colorless oil (1.57 g, 71%). Compound 11 (124.2 mg) was subjected to hydrolysis in 4 M HCl in dioxane (6.0 mL) at 23 °C for 5 h. Removal of the volatiles gave 11-HCl as fine colorless needles (quant.). ¹H NMR matched the literature values.³³

4.11. Hydrolysis of Didemnin B and Derivatization of N,O-Dimethyltyrosine with L- and D-FDTA. A sample of didemnin B (1a, 1.0 mg) was subjected to acid hydrolysis (6 M HCl, 110 °C, ~16 h). The sample was cooled to 23 °C, and the volatiles were removed under a stream of N₂. The mixture was derivatized with L- or D-FDTA (4) as described above. After centrifugation, an aliquot of the supernatant (20 μL) was analyzed by LCMS. t_R (min) and m/z [M + H]⁺ of DTA derivatives 4a: t_R (min, m/z [M + H]⁺), AA = L-Thr (10.14, m/z 487.10), L-Pro (13.55, m/z 483.19), D-N-Me-Leu (21.57, m/z 512.92), L-Leu (18.21, m/z 499.18), L-N,O-Me₂-Tyr (18.40, m/z 577.18). For the t_R values of standard AA-L-DAA (2a) and D-DTA derivatives (4a), see Table 4.

4.12. DFT Calculations of L-Alaninyl-DTA 10 and Its Ammonium Salt 10•NH₄⁺. Optimized geometry and energy of L-alaninyl-DTA (4a R = Me, 10) and the corresponding ammonium salt, 10•NH₄⁺, were calculated using DFT (functional and basis set ωB97X-D, 6-31G*, polar solvent, Spartan '20 Wave function Inc., Irvine, CA, USA). See Supporting Information for results and citation.

■ ASSOCIATED CONTENT

Data Availability Statement

The data underlying this study are available in the published article and its Supporting Information.

Supporting Information

The Supporting Information is available free of charge on the ACS Publications Web site at DOI: xxxx The Supporting Information is available free of charge at <https://pubs.acs.org/doi/10.1021/acs.joc.4c02882>.

¹H and ¹³C NMR of 3 and DFT-calculated structure of 10•NH₄⁺ salt (PDF)

■ AUTHOR INFORMATION

Corresponding Author

Tadeusz F. Molinski – Department of Chemistry and Biochemistry, University of California, San Diego, La Jolla, California 92093-0358, United States; Skaggs School of Pharmacy and Pharmaceutical Sciences, University of California, San Diego, La Jolla, California 92093-0358, United States; orcid.org/0000-0003-1935-2535; Email: tmolinski@uscd.edu.

Author

Mariam N. Salib – Department of Chemistry and Biochemistry, University of California, San Diego, La Jolla, California 92093-0358, United States; orcid.org/0000-0001-9248-0782

Complete contact information is available at:

<https://pubs.acs.org/10.1021/acs.joc.4c02882>

Notes

The authors declare no competing financial interest.

ACKNOWLEDGMENTS

We thank H. Mirahmadi for assistance with extraction–purification of Naproxen, K. Bailey for assistance with marine invertebrate collections, Y. Su (UCSD) for HRMS data, A. Mrse and B. Duggan (UCSD) for assistance with NMR measurements, and J. Pawlik (UNC Wilmington) and the crew of the RV Seward Johnson for collection logistics in the Bahamas. The 500 MHz NMR spectrometer and the HPLC TOFMS were purchased with funding from the NSF (Chemical Research Instrument Fund, CHE0741968) and the NIH Shared Instrument Grant (S10RR025636) programs, respectively. This work was supported by a grant from NIH (R01 AI1007786).

REFERENCES

- (1) Marfey, P. Determination of D-Amino Acids. II. Use of a Bifunctional Reagent, 1,5-Difluoro-2,4-dinitrobenzene. *Carlsberg Res. Commun.* **1984**, *49*, 591.
- (2) (a) Rinehart, K. L., Jr.; Gloer, J. B.; Cook, J. C., Jr.; Mizsak, S. A.; Scabill, T. A. Structures of the Didemnins, Antiviral and Cytotoxic Depsipeptides from a Caribbean tunicate. *J. Am. Chem. Soc.* **1981**, *103*, 1857–1859. (b) Sakai, R.; Stroh, J. G.; Sullins, D. W.; Rinehart, K. L. Seven New Didemnins from the Marine Tunicate *Trididemnum solidum*. *J. Am. Chem. Soc.* **1995**, *117*, 3734–3748. (c) Rinehart, K.; Gloer, J.; Hughes, R.; Renis, H.; McGovern, J.; Swynenberg, E.; Stringfellow, D.; Kuentzel, S.; Li, L. Didemnins: antiviral and antitumor depsipeptides from a caribbean tunicate. *Science* **1981**, *212*, 933–935. (d) Rinehart, K. L. U.S. Patent 5,294,603 A, Mar 15, 1994. (e) Rinehart, K. L.; Lithgow-Bertelloni, A. M.. WO 1991004985 A1, Apr 18, 1991.
- (3) Leisch, M.; Egle, A.; Greil, R. Plitidepsin: a potential new treatment for relapsed/refractory multiple myeloma. *Future Oncol.* **2019**, *15*, 109–120.
- (4) Vervoort, H.; Fenical, W.; Epifanio, R. de A. Tamandarins A and B: New Cytotoxic Depsipeptides from a Brazilian Ascidian of the Family Didemnidae. *J. Org. Chem.* **2000**, *65*, 782–792.
- (5) While didemnin B. (**1a**) fell out of human trials, Aplidin® (dehydrodidemnin B, **1b**) was successfully advanced through phase III clinical trials; it is now granted 'orphan status' in the EU for acute lymphoblastic leukemia and has been approved in Australia for multiple myeloma. <https://myelomaresearchnews.com/2019/01/04/aplidin-approved-in-australia-for-relapsed-or-refractory-multiple-myeloma/>. Accessed February 12, 2025
- (6) Varona, J. F.; Landete, P.; Lopez-Martin, J. A.; Estrada, V.; Paredes, R.; Guisado-Vasco, P.; Fernandez de Orueta, L.; Torralba, M.; Fortun, J.; Vates, R.; Barberan, J.; Clotet, B.; Ancochea, J.; Carnevali, D.; Cabello, N.; Porras, L.; Gijon, P.; Monereo, A.; Abad, D.; Zuñiga, S.; Sola, I.; Rodon, J.; Vergara-Alert, J.; Izquierdo-Useros, N.; Fudio, S.; Pontes, M. J.; de Rivas, B.; Giron de Velasco, P.; Nieto, A.; Gomez, J.; Aviles, P.; Lubomirov, R.; Belgrano, A.; Sopesen, B.; White, K. M.; Rosales, R.; Yildiz, S.; Reuschl, A. K.; Thorne, L. G.; Jolly, C.; Towers, G. J.; Zuliani-Alvarez, L.; Bouhaddou, M.; Obernier, K.; McGovern, B. L.; Rodriguez, M. L.; Enjuanes, L.; Fernandez-Sousa, J. M.; Krogan, N. J.; Jimeno, J. M.; Garcia-Sastre, A. Preclinical and randomized phase I studies of plitidepsin in adults hospitalized with COVID-19. *Life Sci. Alliance* **2022**, *5*, No. e202101200.
- (7) Bhushan, R.; Brückner, H. *Amino Acids* **2004**, *27*, 231–247.
- (8) Fujii, K.; Ikai, Y.; Mayumi, T.; Oka, H.; Suzuki, M.; Harada, K.-I. A Nonempirical Method Using LC/MS for Determination of the Absolute Configuration of Constituent Amino Acids in a Peptide: Elucidation of Limitations of Marfey's Method and of its Separation Mechanism. *Anal. Chem.* **1997**, *69*, 3346–3352.
- (9) Bhushan, R.; Kumar, V. Synthesis and Application of New Chiral Variants of Marfey's Reagent for Liquid Chromatographic Separation of the Enantiomers of α -Amino Acids. *Acta Chromatica* **2008**, *3*, 329–347.
- (10) Brückner, H.; Keller-Hoehl, C. HPLC separation of DL-amino acids derivatized with N^2 -(5-fluoro-2,4-dinitrophenyl)-1-amino acid amides. *Chromatographia* **1990**, *30*, 621–629.
- (11) Kotthaus, A. F.; Altenbach, H.-J. A new chiral derivatizing agent for the HPLC separation of α -amino acids on a standard reverse-phase column. *Amino Acids* **2011**, *40*, 527–532.
- (12) Sethi, S.; Martens, J.; Bhushan, R. Assessment and application of Marfey's reagent and analogs in enantioseparation: a decade's perspective. *Biomed. Chromatogr.* **2021**, *35*, No. e4990.
- (13) Bhushan, R.; R Brückner, H. Use of Marfey's reagent and analogs for chiral amino acid analysis: Assessment and applications to natural products and biological systems. *J. Chromatogr. B: Anal. Technol. Biomed. Life Sci.* **2011**, *879*, 3148–3161.
- (14) B'Hymer, C. B.; Montes-Bayon, M.; Caruso, J. A. Marfey's reagent: Past, present, and future uses of 1-fluoro-2,4-dinitrophenyl-5-L-alanine amide. *J. Sep. Sci.* **2003**, *26*, 7–19.
- (15) Fernandes, C.; Ribeiro, R.; Pinto, M.; Kijjoa, A. Absolute Stereochemistry Determination of Bioactive Marine-Derived Cyclopeptides by Liquid Chromatography Methods: An Update Review (2018–2022). *Molecules* **2023**, *28*, 615–6157.
- (16) Dalisay, D. S.; Rogers, E. W.; Edison, A. S.; Molinski, T. F. Structure Elucidation at the Nanomole Scale. 1. Trisoxazole Macrolides and Thiazole-Containing Cyclic Peptides from the Nudibranch *Hexabranchnus sanguineus*. *J. Nat. Prod.* **2009**, *72*, 732–738.
- (17) Vijayasathy, S.; Prasad, P.; Fremlin, L. J.; Ratnayake, R.; Salim, A. A.; Khalil, Z.; Capon, R. J. C₃ and 2D C₃ Marfey's Methods for Amino Acid Analysis in Natural Products. *J. Nat. Prod.* **2016**, *79*, 421–427.
- (18) Salib, M. N.; Molinski, T. F. Cyclic Hexapeptide Dimers, Antatollamides A and B, from the Ascidian, *Didemnum molle*. A Tryptophan-Derived Auxillary for L- and D-Amino Acid Assignments. *J. Org. Chem.* **2017**, *82*, 10181–10187.
- (19) Martin, E.; Quinke, K.; Spahn, H.; Mutschler, E. (–)-(S)-Flunoxapfen and (–)-(S)-naproxen isocyanate: Two new fluorescent chiral derivatizing agents for an enantiospecific determination of primary and secondary amines. *Chirality* **1989**, *1*, 223–234.
- (20) From the outset, we had hoped the aromatic rings in L-Trp and (S)-Naproxen would lend their inherent fluorescence ($\lambda_{em} = 295$ and 360 nm, respectively) to the reagents (S)-**3** and L-**4** as an added advantage to enhance sensitivity in detection. Upon measurement of fluorescence spectra, emissions of the two compounds were observed to be only marginal, most likely due to efficient intramolecular quenching by the dinitrophenyl group.
- (21) Harada, K.-I.; Fujii, K.; Mayumi, T.; Hibino, Y.; Suzuki, M.; Ikai, Y.; Oka, H. A method using L/CMS for Determination of Absolute Configuration of Constituent Amino Acids in Peptide — Advanced Marfey's method —. *Tetrahedron Lett.* **1995**, *36*, 1515–1518.
- (22) Fujii, K.; Shimoya, T.; Ikai, Y.; Oka, H.; Harada, K.-I. Further application of advanced Marfey's method for determination of absolute configuration of primary amino compound. *Tetrahedron Lett.* **1998**, *39*, 2579–2582.
- (23) In our own extensive experience with derivatization of AAs with FDDA conducted under standard condition (85 °C), and now with FDTA, we've only ever observed partial diastereomerization for two AAs: Ser and the uncommon 2,3-diaminopropionic acid (DAP) where it occurs to the extents of < 5% and ~10%, respectively. Both likely are due to inductive effects of the β -NH₂ or β -HO upon the pK_a of the α -CH.
- (24) Separations of L-DAA and S-DTA derivatives of the diastereomeric L-Ile and D-*allo*-Ile (Table 4)—a common encounter in natural product peptides—were $\Delta t_R = 3.13$ and 3.49 min, respectively, on a conventional column (Table 4, C₁₈, 3 μ m). The critical separation L-Ile-DTA and *allo*-L-Ile-DTA dramatically

improved with a UHPLC column (Table 3, particle size = 1.9 μm , Δt_{R} = 1.03 min) compared to a conventional column. Both L-DAA and L-DTA derivatives of enantiomeric L- and D-Ile were well separated (Δt_{R} = 3.16 and 3.33 min, respectively, Table 4).

(25) The use of the term 'buffer' for aqueous NH_4OAc solutions in LC-ESIMS is contentious and possibly a misnomer. Konermann, L. Addressing a Common Misconception: Ammonium Acetate as Neutral pH "Buffer" for Native Electrospray Mass Spectrometry. *J. Am. Soc. Mass Spectrom.* **2017**, *28*, 1827–1835.

(26) Bruckner, H.; Gah, C. High-performance liquid chromatographic separation of DL- amino acids derivatized with chiral variants of Sanger's reagent. *J. Chromatogr.* **1991**, *555*, 81–95.

(27) Kennedy, C. R.; Lin, S.; Jacobsen, E. N. The Cation– π Interaction in Small-Molecule Catalysis. *Angew. Chem., Int. Ed.* **2016**, *55*, 12596.

(28) A full report will be disclosed in due course.

(29) Molinski, T. F.; Ko, J.; Reynolds, K. A.; Lievens, S. C.; Skarda, K. R. N,N'-Methylene-didemnin A from the Ascidian *Trididemnum solidum*. Complete NMR Assignments and Confirmation of the Imidazolidinone Ring by Strategic Analysis of $^1J_{\text{CH}}$. *J. Nat. Prod.* **2011**, *74*, 882–887.

(30) *The Merck Index*, 12th ed.; Budavari, S., M. J., O'Neil, Smith, A., Heckelman, P. E., Kinneary, J. F., Eds.; Merck Research Laboratories: Whitehouse Station, NJ, 1996.

(31) https://hmdb.ca/spectra/nmr_one_d/1802. Accessed February 12, 2025.

(32) Spahn, H.; Langguth, P. Chiral Amines Derived from 2-Arylpropionic Acids: Novel Reagents for the Liquid Chromatographic (LC) Fluorescence Assay of Optically Active Carboxylic Acid Xenobiotics. *Pharm. Res.* **1990**, *12*, 1262–1268.

(33) Marner, F.-J.; Moore, R. E.; Hirotsu, K.; Clardy, J. Majusculamides, A and B Two Epimeric Lipodipeptides from *Lyngbya majuscula* Gomont. *J. Org. Chem.* **1977**, *42*, 2815–2819.